# Removal of tetracycline antibiotic from contaminated water media by multi-walled carbon nanotubes: operational variables, kinetics, and equilibrium studies

Ali Akbar Babaei, Eder C. Lima, Afshin Takdastan, Nadali Alavi, Gholamreza Goudarzi, Mehdi Vosoughi, Ghasem Hassani and Mohammad Shirmardi

## ABSTRACT

Multi-walled carbon nanotubes (MWCNTs) were purified and oxidized by a 4 mol $L^{-1}$ mixture of $H_2SO_4$:$H_2O_2$ and then were used as adsorbent for tetracycline (TC) adsorption from aqueous solutions. The purified MWCNTs were characterized using Fourier transform infrared spectroscopy, field emission scanning electron microscopy, energy dispersive X-ray spectroscopy, X-ray diffraction, and $N_2$ adsorption/desorption isotherms. The adsorption of TC onto the MWCNT was investigated as a function of the initial pH of the solution, adsorbent dosage, and background electrolyte cations and anions. The results of the one-way analysis of variance (ANOVA) showed that $Fe^{3+}$ ion significantly affected and decreased TC adsorption onto the MWCNT ($P$-value $< 0.05$), while other studied cations and anions did not affect TC adsorption ($P$-value $> 0.05$). Nonlinear pseudo-first-order, pseudo-second-order, general order, and Avrami fractionary-order kinetic models were used to investigate the kinetics of TC adsorption. The fractionary-order kinetic model provided the best fit to experimental data. In addition, the adsorption isotherms data were well described by nonlinear equation of the Liu isotherm model with the maximum adsorption capacity of 253.38 mg $g^{-1}$. The results of this study indicate that the oxidized MWCNTs can be used as an effective adsorbent for TC removal from aqueous solutions.

**Key words** | adsorption, antibiotics, carbon nanotubes, nonlinear kinetics and isotherms modeling, tetracycline

**Ali Akbar Babaei**
**Afshin Takdastan**
**Gholamreza Goudarzi**
**Mehdi Vosoughi**
**Mohammad Shirmardi** (corresponding author)
Environmental Technologies Research Center (ETRC),
Ahvaz Jundishapur University of Medical Sciences,
Ahvaz, Iran
and
Department of Environmental Health Engineering,
School of Public Health, Ahvaz Jundishapur University of Medical Sciences,
Ahvaz, Iran
E-mail: *shirmardim@yahoo.com*

**Eder C. Lima**
Institute of Chemistry,
Federal University of Rio Grande do Sul (UFRGS),
Av. Bento Gonçalves 9500,
Porto Alegre, RS, Brazil

**Nadali Alavi**
Environmental and Occupational Hazards Control Research Center,
Shahid Beheshti University of Medical Sciences,
Tehran, Iran
and
Department of Environmental Health Engineering,
School of Public Health, Shahid Beheshti University of Medical Sciences,
Tehran, Iran

**Mehdi Vosoughi**
**Mohammad Shirmardi**
Student Research Committee,
Ahvaz Jundishapur University of Medical Sciences,
Ahvaz, Iran

**Ghasem Hassani**
Department of Environmental Health Engineering,
School of Public Health, Yasuj University of Medical Sciences,
Yasuj, Iran

## INTRODUCTION

Traditionally, the chemical compounds used for eradicating or inhibiting the growth of microorganisms are known as antibiotics. However, this term also includes antibacterial, antiviral, antifungal, and antitumor compounds (Homem & Santos 2011). In recent years, pharmaceutical antibiotics, due to their great therapeutic values, are widely used in human therapy to prevent infections. They are also used in the livestock and farming industries against disease-producing bacteria, and for growth rate promotion (Zhao *et al.* 2012; Safari *et al.* 2015). The extensive and indiscriminate use of pharmaceutical antibiotics has raised significant concerns because they have the potential to create adverse

doi: 10.2166/wst.2016.301

effects such as acute and chronic toxicity. Additionally, they affect aquatic photosynthetic organisms and disrupt indigenous microbial populations. The emergence of new strains of bacteria, which are resistant to these antibiotics, is another major concern. This, in turn, may result in untreatable livestock diseases. Subsequently, possible transmission of such strains to humans may lead to untreatable human diseases (Homem & Santos 2011; Gao *et al.* 2012; Zhao *et al.* 2012).

Since a small portion of most antibiotics, including tetracycline (TC), could be metabolized or absorbed by the body of a treated human or animal, large fractions of these substances are excreted through urine and feces as unchanged parent compounds (Gao *et al.* 2012; Kyzas *et al.* 2015). Antibiotics can be released into the environment from many sources such as effluents from municipal wastewater treatment plants and effluents from pharmaceutical manufacturing plants because conventional water and wastewater treatment technologies cannot remove antibiotics completely. The application of animals' manure and sewage sludge to agricultural fields, as fertilizers, is another major source that release antibiotics into the environment through runoff, leaching, and other ways. Residues of these antibiotics discharged from above-mentioned sources are frequently detected in soil, surface water, groundwater, and even drinking water (Zhang *et al.* 2011c; Thayyath *et al.* 2015; Terzopoulou *et al.* 2016).

Thus, to prevent and minimize the risks related to antibiotics, effluent-containing antibiotics must be treated by an appropriate technique. Several methods have been evaluated to remove antibiotics from aqueous solutions, including conventional techniques (biological process, filtration, coagulation, flocculation and sedimentation), advanced oxidation process ($AOP_S$), membrane treatment, adsorption, and combined methods (Homem & Santos 2011; Jaafarzadeh *et al.* 2015; Ma *et al.* 2015; Kakavandi *et al.* 2016). Each of these methods has different removal efficiency, capital costs, advantage, disadvantage, and operating rates. Previous studies (Homem & Santos 2011; Kakavandi *et al.* 2014) reported that physical techniques, particularly adsorption, are appropriate and more efficient than chemical processes for the removal of recalcitrant and organic compounds. In addition, the adsorption method can produce a high quality effluent without the presence of hazardous substances (Shirmardi *et al.* 2013b; Vosoughi Niri *et al.* 2014). The adsorption of TC has been evaluated by several materials as adsorbent including bamboo charcoal (Liao *et al.* 2013), montmorillonite (Zhao *et al.* 2012), bio-char (Liu *et al.* 2012b), graphene oxide (Gao *et al.* 2012), soil and sediment (Zhang *et al.* 2011c), activated carbon (Martins *et al.* 2015; Zhang *et al.* 2015), multi-walled carbon nanotubes (MWCNTs) (Zhang *et al.* 2011b) and single-walled carbon nanotubes (Ji *et al.* 2009). Carbon nanotubes, due to their relatively large specific surface areas, unique hollow and porous structure, high mechanical strength, small size and remarkable electrical conductivities, have been utilized as a new and promising adsorbent to remove many kinds of organic and inorganic contaminants (Shirmardi *et al.* 2012; Yu *et al.* 2014a; Babaei *et al.* 2015). For instance, Yu *et al.* (2016) investigated the adsorptive removal of ciprofloxacin (CPX) by MWCNTs with different oxygen contents. The authors reported that with increasing the oxygen content of the MWCNT from 2.0% to 5.9%, the normalized maximum adsorption capacity of CPX increases. Zhang *et al.* (2011a) evaluated the adsorption of sulfamethoxazole (SMX) on functionalized carbon nanotubes and reported that various mechanisms such as electrostatic interaction, hydrophobic interaction, π-π, and hydrogen bonds play roles in SMX adsorption. It should be pointed out that surface chemical functionalization of MWCNT could improve its adsorptive capacity by introducing various functional groups as well as providing new adsorption sites for the adsorption of target pollutants. Additionally, the hydrophobicity of CNTs can be decreased by functional groups; consequently, the adsorption of organic compounds with relatively low molecular weight and polar properties increases considerably. Despite of the availability of different modification methods, oxidation has been proved as a simple method for producing hydroxyl and carbonyl groups to the sidewalls of CNTs (Zhang *et al.* 2011a; Yu *et al.* 2014b). In this study, since MWCNTs have not been oxidized by a mixture of $H_2SO_4$:$H_2O_2$ for the adsorption of TC from the aqueous solutions, we first oxidized and purified the MWCNT and then investigated its efficiency for TC adsorption. The effects of basic variables such as pH of solution, MWCNT dosage, background electrolytes, contact time, and initial concentration on the adsorption of TC were evaluated. The kinetics and isotherms of adsorption of TC on MWCNT were also investigated.

## MATERIALS AND METHODS

### Reagents and solutions

The analytical high performance liquid chromatography (HPLC) grade TC with the purity of ≥88% was purchased from Sigma-Aldrich Chemical Co. (USA), and was used

without further purification. The chemical structure and some main characteristics of TC are presented in Table 1. Methanol and acetonitrile (both HPLC grade), and oxalic acid dehydrate were purchased from Merck company, Germany. MWCNTs were purchased from the Iranian Research Institute of Petroleum Industry (IRIPI). These CNTs were synthesized in the $CH_4/H_2$ mixture at 700 °C by a chemical vapor deposition method using Co-Mo particles as catalysts. The method of synthesis has been previously described in the literature (Dehghani *et al.* 2013; Derakhshani & Naghizadeh 2013). The diameter and the length of the MWCNT were in the range of 10–30 nm and 10 μm, respectively. In addition, the purity of the CNTs was more than 95%. All above-mentioned information was provided by the IRIPI.

Deionized water was used throughout the experiments to prepare working solutions. The stock solution of TC was prepared freshly by weighing and dissolving the desired amount of TC in deionized water, and was kept in the dark below 4 °C. The required concentrations for the experiments were obtained by diluting the stock solution to 100 mL, brown, volumetric flasks.

All other chemicals used were analytical reagent grade and were used without further purification.

## Treatment and characterization of the adsorbent

In order to oxidize, purify, and remove the amorphous carbon and Co-Mo catalysts from the MWCNT, 4 g of the as-received MWCNT were immersed in 200 mL mixture of $H_2SO_4$:$H_2O_2$ (both 4 mol $L^{-1}$) with the volumetric ratio of 70:30. The mixture was then heated and refluxed at 120 °C for 2 h under continuous magnetic stirring. Afterwards, the mixture was filtrated and washed with deionized water several times until the pH of the suspension reached about 6, and then was dried at 80 °C in an oven overnight.

The treated MWCNTs were characterized using Fourier transform infrared spectroscopy (FTIR) (Perkin-Elmer Spectrum One) to identify the surface functional groups of the oxidized MWCNT. The MWCNT and KBr were previously dried at 120 °C for 8 h, stored in a capped flask, and kept in a desiccator before performing the analysis (Ribas *et al.* 2014). The spectra are recorded for the MWCNT sample in the spectral range of 4,000–400 $cm^{-1}$.

The MWCNT was also characterized by employing field emission scanning electron microscope (FESEM, model Mira 3-XMU) to observe surface morphologies of the adsorbent. The FESEM device was equipped with an energy dispersive X-ray spectrometer (EDS) analyzer; thus, we performed the EDS analysis to identify the elemental composition of the MWCNT. The adsorbent was also characterized by X-ray diffraction (XRD) with a Philips Xpert MPD diffractometer (The Netherlands) operating at 40 kV and 40 mA with Cu Kα radiation (λ = 1.5406 Å). Measurements were done with scanning step width of 0.02 ° and time of 3 s, over the 2$\theta$ range of 10–90 °.

The $N_2$ adsorption–desorption isotherms of the MWCNT were carried out at liquid nitrogen boiling point (77 K) using a surface analyzer. Before the analysis, the sample was degassed for 4 h at 300 °C under vacuum. The specific surface area, pore size and volume of the adsorbent were evaluated using the Brunauer, Emmett, and Teller multipoint technique and the Barrett, Joyner, and Halenda method, respectively (Machado *et al.* 2012).

## Adsorption experiments

To investigate the adsorption of TC onto the MWCNT, batch adsorption experiments were carried out using a series of 100 mL, brown, volumetric flasks containing 50 mL TC solution of known concentration. We used this type of flask to prevent possible light degradation of TC. The flasks were then transferred into an incubator shaker and agitated at 200 rpm at 20 °C. A series of adsorption experiments were performed to evaluate the effects of operational parameters such as solution pH, adsorbent dosage, background electrolytes, contact time, and initial concentration of TC. In addition, the adsorption kinetics and isotherms were analyzed. The experimental solutions with different initial concentrations were obtained by diluting the stock solution in the required proportions.

**Table 1** | Chemical structure and main characteristics of TC antibiotic

| Name | Chemical formula | Molecular weight | Molecular structure | $pK_{a1}$ | $pK_{a2}$ | $pK_{a3}$ |
|---|---|---|---|---|---|---|
| TC | $C_{22}H_{24}N_2O_8{\cdot}xH_2O$ | 444.43 | 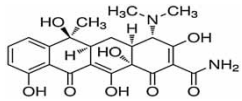 | 3.3 | 7.68 | 9.68 |

### Effect of solution pH

The first step in this work was to study the effect of pH on TC adsorption. To determine the optimum pH at which maximum adsorption could be achieved, the initial pH of the solutions (50 mL, initial concentration 50 mg $L^{-1}$) was adjusted from 3 to 11 using 0.1 mol $L^{-1}$ HCl or NaOH. The adsorbent dosage and the agitation time were 0.5 g $L^{-1}$ and 4 h, respectively. In addition, another set of brown flasks containing the same concentrations of TC without the adsorbent were used as blanks to investigate whether pH of the adsorbate solution would have some effect on TC adsorption.

### Effect of MWCNT dosage

The MWCNT at different dosages (0.1, 0.25, 0.5, 0.75, and 1 g $L^{-1}$) were added to the flasks containing two initial TC concentrations of 50 and 100 mg $L^{-1}$. The other variables such as the contact time and solution pH were fixed at 4 h and the natural pH of the solutions, respectively.

### Effect of anions and cations on the adsorption

In order to study the effects of different anions and cations on the adsorption of TC, 1 g $L^{-1}$ of the MWCNT was added to the solutions containing 1 mM sodium salts of nitrate, bicarbonate, and sulfate anions or chloride salts of cations such as potassium, magnesium, nickel, lithium, and ferric ions. In addition, the initial TC concentration and pH of the solutions were 100 mg $L^{-1}$ and natural pH, respectively. Other parameters were kept constant. One-way analysis of variance (ANOVA) test was used to compare the results of this run.

### Effect of contact time and kinetic studies

The experiments for investigating the effect of contact time and adsorption kinetics were carried out by adding 1 g $L^{-1}$ of the adsorbent into the initial TC concentration of 75 and 100 mg $L^{-1}$. The contact time ranged from 5 to 420 min, and when the predetermined time elapsed, the sample was withdrawn and filtered using a syringe membrane filter with the pore size of 0.22 μm. The filtrate was kept in a refrigerator below 4 °C before the measurement of the residual TC concentration. It is worth noting that in this stage of the study, pH was the natural pH (close to 4.71) of the prepared solutions. For kinetics study, nonlinear pseudo-first-order, pseudo-second-order, general-order, Avrami fractionary-order kinetic models, and intra-particle diffusion model were employed to fit the kinetic data. These models are given by Equations (1)–(5), respectively (Weber & Morris 1963; Ho 2006; Liu & Liu 2008; Liu & Shen 2008; Cardoso *et al.* 2011; Machado *et al.* 2012).

$$q_t = q_e.[1 - \exp(-k_f.t)] \tag{1}$$

$$q_t = \frac{k_s \times q_e^2 \times t}{1 + q_e \times k_s \times t} \tag{2}$$

$$q_t = q_e - \frac{q_e}{[k_N (q_e)^{n-1} \times t \times (n-1) + 1]^{1/1-n}} \tag{3}$$

$$q_t = q_e \times \{1 - \exp[-(k_{AV} \times t)]^{n_{AV}}\} \tag{4}$$

$$q_t = k_{id}\sqrt{t} + C \tag{5}$$

where $t$ is the contact time (min); $q_t$ is the amount of adsorbate (TC in this study) adsorbed at time $t$ (mg $g^{-1}$); $q_e$ is the amount of adsorbate adsorbed at the equilibrium (mg $g^{-1}$); $k_f$ is the pseudo-first-order rate constant ($min^{-1}$); $k_s$ is the pseudo-second-order rate constant (g $mg^{-1}min^{-1}$); $k_N$ is the general order rate constant [$min^{-1}\times$ (g $mg^{-1})^{n-1}$]; $n$ is the order of kinetic adsorption ($n$ could be an integral or a fractional number). $k_{AV}$ is the Avrami kinetic constant ($min^{-1}$); $n_{AV}$ is a fractionary reaction order (Avrami) which can be related to the adsorption mechanism.

### Equilibrium studies

To obtain the adsorption isotherms, 1 g $L^{-1}$ of the MWCNT were added to TC solutions with the concentration ranging from 10 mg $L^{-1}$ to 300 mg $L^{-1}$ at contact time 4 h, temperature 20 °C, and natural pH. In this work, nonlinear equations of the Langmuir (Langmuir 1918), Freundlich (Freundlich 1906), Liu (Liu *et al.* 2003), and Redlich–Peterson (Redlich & Peterson 1959) isotherm models, as respectively shown in Equations (6)–(9), were used to fit the experimental data. These models are widely used to fit the adsorption of various contaminants on carbon-based adsorbents such as CNTs (Shirmardi *et al.* 2013a), activated carbon (Saucier *et al.* 2015a) and biochars (Mohan *et al.* 2011).

$$q_e = \frac{Q_{\max} \times K_L \times C_e}{1 + K_L \times C_e} \tag{6}$$

$$q_e = K_F \times C_e^{1/n_F} \tag{7}$$

$$q_e = \frac{Q_{\max} \times (K_g \times C_e)^{n_L}}{1 + (K_g \times C_e)^{n_L}} \quad (8)$$

$$q_e = \frac{K_{RP} \times C_e}{1 + a_{RP} \times C_e^g} \quad \text{where} \quad 0 < g \leq 1 \quad (9)$$

where $q_e$ is the amount of adsorbate (TC) adsorbed at the equilibrium (mg $g^{-1}$); $C_e$ is the equilibrium concentration of the adsorbate (mg $L^{-1}$); $Q_{max}$ is the maximum adsorption capacity of the adsorbent (mg $g^{-1}$); $K_L$ is the Langmuir equilibrium constant (L $mg^{-1}$); $K_F$ is the Freundlich equilibrium constant [mg $g^{-1}$× (mg $L^{-1}$)$_F^{-1/n}$]; $K_g$ is the Liu equilibrium constant (L $mg^{-1}$); $n_F$ and $n_L$ are the dimensionless exponents of the Freundlich and Liu models, respectively. $K_{RP}$ and $a_{RP}$ are Redlich–Peterson constants with the respective units of L $g^{-1}$ and (mg $L^{-1}$)$^{-g}$, and $g$ is the Redlich–Peterson exponent (dimensionless), whose value should be $\leq 1$.

### TC determination

At the end of each run, after filtering, the residual concentration of TC in the solution was analyzed by a Knauer HPLC instrument, equipped with a Eurospher column (5 μm 4.6 mm × 250 mm) and an ultimate variable wavelength UV detection 2500, at a wavelength of 360 nm. The column temperature, the injection volume of the sample, and the flow rate were 35 °C, 100 μL, and 1 mL $min^{-1}$, respectively. The mobile phase used for elution was a mixture of oxalic acid (0.01 M): methanol:acetonitrile with a volumetric ratio of 70:20:10. The residual concentration of TC in the solutions was calculated from the areas under the curves extrapolated automatically by the software. The standards of TC (initial concentration of 0.01, 0.1, 1, 5, 10, 20, 50, and 100 mg $L^{-1}$) were prepared and analyzed by the HPLC at operating conditions to form the calibration curve. The determination coefficient ($R^2$) for TC was obtained to be 0.9999. The retention time of TC was about 6.7 min. The same procedure has been used by other researchers for TC determination (Liu *et al.* 2012a; Alavi *et al.* 2015).

The TC removal percentage, the amounts of TC adsorbed at time $t$ ($q_t$, mg $g^{-1}$) and at equilibrium ($q_e$, mg $g^{-1}$) were calculated through the following equations, respectively (Shirmardi *et al.* 2013a, 2013b):

$$\text{TC removal } \% = \frac{(C_o - C_e)}{C_o} \times 100 \quad (10)$$

$$q_t = \frac{(C_o - C_t) \times V}{M} \quad (11)$$

$$q_e = \frac{(C_o - C_e) \times V}{M} \quad (12)$$

where $C_o$ and $C_e$ (mg $L^{-1}$) are the initial and equilibrium concentrations of TC in the solution; $M$ (g) is the mass of MWCNT, $V$ (L) is the volume of the solution, and $C_t$ (mg $L^{-1}$) and $q_t$ (mg $g^{-1}$) are the concentration of TC at time $t$ and the amount of TC adsorbed onto MWCNT at time $t$, respectively.

### Statistical evaluation of kinetic and isotherm parameters

In this work, the kinetic and equilibrium data were fitted by employing a nonlinear method, with successive interactions calculated by the Levenberg–Marquardt method. Interactions were also calculated using the Simplex method based on the nonlinear fitting facilities of the OriginPro 2015 software. The suitability of the models was evaluated using a determination coefficient ($R^2$), an adjusted determination coefficient ($R^2_{adj}$) and a standard deviation (SD). The SD is a measurement of the difference between the theoretical value of $q$ predicted by the model and the actual $q$ measured experimentally. The respective mathematical expressions of $R^2$, $R^2_{adj}$ and SD are respectively given below by Equations (13)–(15).

$$R^2 = \left( \frac{\sum_i^n (q_{i,\exp} - \bar{q}_{\exp})^2 - \sum_i^n (q_{i,\exp} - q_{i,model})^2}{\sum_i^n (q_{i,\exp} - \bar{q}_{\exp})^2} \right) \quad (13)$$

$$R^2_{adj} = 1 - (1 - R^2) \times \left( \frac{n-1}{n-p-1} \right) \quad (14)$$

$$SD = \sqrt{\left( \frac{1}{n-p} \right) \times \sum_i^n (q_{i,\exp} - q_{i,\text{model}})^2} \quad (15)$$

In these equations, $q_{i,\exp}$ represents individual value of q measured experimentally; $q_{i,\text{model}}$ represents individual value of q predicted by the model fitted; $\bar{q}_{\exp}$ represents the average value of all $q$ measured experimentally; $n$ is the number of experiments performed; $p$ represents the number of parameters of the fitted model (Saucier *et al.* 2015b).

## RESULTS AND DISCUSSION

### Characterization of the adsorbent

Figure 1 shows the FTIR vibrational spectrum of the MWCNT. The FTIR spectrum of the oxidized MWCNT

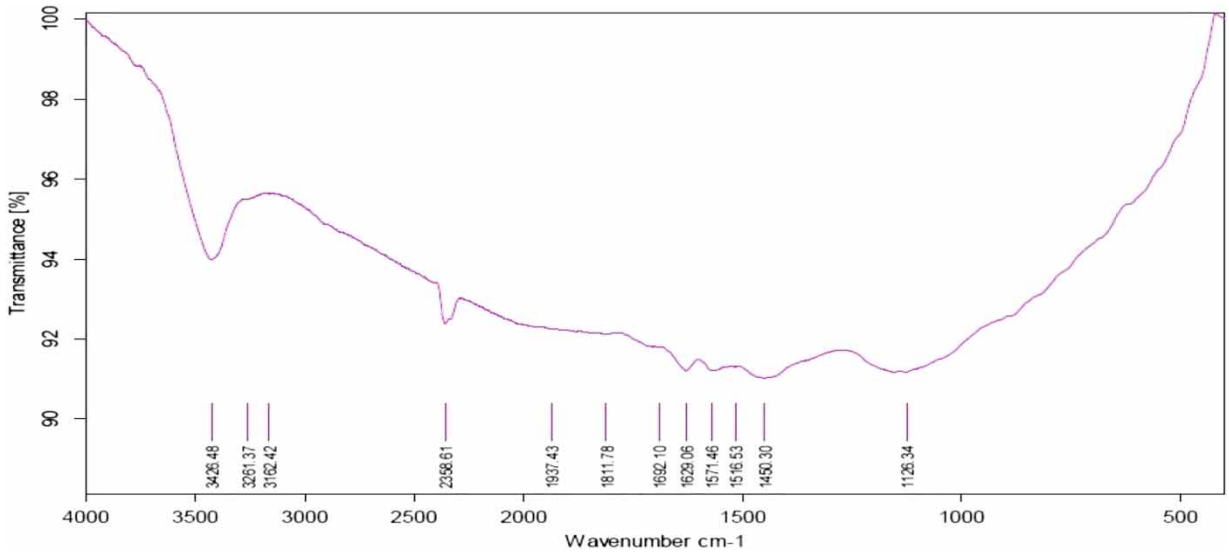


**Figure 1** | FTIR spectrum of the oxidized MWCNT.

shows a broad band at 3,426 $cm^{-1}$, which refers to the OH stretching of the hydroxyl group, coming from acid treatment process. The band at 2,358 $cm^{-1}$ can be associated with the OH stretching from strongly hydrogen bonded -COOH group (Morsy *et al.* 2014). The peaks observed at 1,571 and 1,630 $cm^{-1}$ were assigned to C=C stretch and carbonyl group C=O, respectively (Machado *et al.* 2012). The peak at 1,450 $cm^{-1}$ represents the C–C vibrational mode associated with the carbon backbone of the MWCNT (Chaudhary *et al.* 2014). The band at 1,129 $cm^{-1}$ was assigned to C–O stretch (Salam & Burk 2008). The FTIR spectrum of the oxidized MWCNT confirms that oxygen-containing functional groups are abundant on the surface of MWCNT. Therefore, the presence of these groups can provide numerous adsorption sites on the surface of the MWCNT for the adsorption of TC molecules. The FESEM images of the oxidized MWCNT at various magnifications are depicted in Figure 2. It is clear that the MWCNT has a tubular shape with the external diameter of 18 nm (Figure 2). The EDS spectrum and the XRD pattern of the MWCNT are shown in Figure 3(a) and 3(b), respectively. The EDS spectrum of the MWCNT shows that C, O, Mo, and Co elements are present in the composition of the MWCNT. Carbon composes 90% (weight percent) and 96% (atomic percent) of the MWCNT. Table 2 presents the quantitative results of EDS analysis of the MWCNT. The XRD pattern of the MWCNT shows a broad peak at position 26.5 ° and several relatively weak peaks at positions 42.5 ° and 44.5 ° for $2\theta$, which can be indexed to carbon (C) phase (JCPDS card 00-026-1077). The other phases that were detected by XRD can be indexed to cobalt (JCPDS card 00-001-1255), molybdenum oxide ($Mo_{18}O_{52}$, JCPDS card 01-074-1664), molybdenum carbide ($Mo_2C$, JCPDS card 01-072-1683), molybdenum carbonyl (Mo(CO) 6, JCPDS card 00-012-0691), cobalt oxide (CoO, JCPDS card 01-075-0418), and cobalt molybdenum oxide ($CoMoO_4$, JCPDS card 00-021-0868) (Figure 3(b)). The textural properties of the MWCNT are presented in Table 3. The relatively large pore diameter of the MWCNT could be attributed to the aggregated pores of the MWCNT. The formation of aggregated pores in the MWCNT is due to the entanglement of tens and hundreds of individual tubes, which are adhered to each other because of van der Waals attraction forces. Therefore, the aggregated pores have the dimensions of a mesopore or higher (Upadhyayula *et al.* 2009; Prola *et al.* 2013).

## Effect of pH of adsorbate solution

The effect of solution pH on the adsorption of TC onto the MWCNT is shown in Figure 4. The solution pH significantly affected TC adsorption onto the MWCNT, mainly for pH values higher than 7. The adsorption percentage increases when the solution pH is increased from 3 to 5; it remains almost unchanged and there is no observable change in the adsorption of TC onto the MWCNT as the solution pH is further increased from 5 to 7. However, TC adsorption percentage decreases considerably as the pH is increased from 7 to 11. The adsorption percentage decreases when the pH is $\leq 3$ or pH $>7$. For the initial TC concentration of 50 mg $L^{-1}$, the removal percentage decreases from 84% to 54% when the solution pH

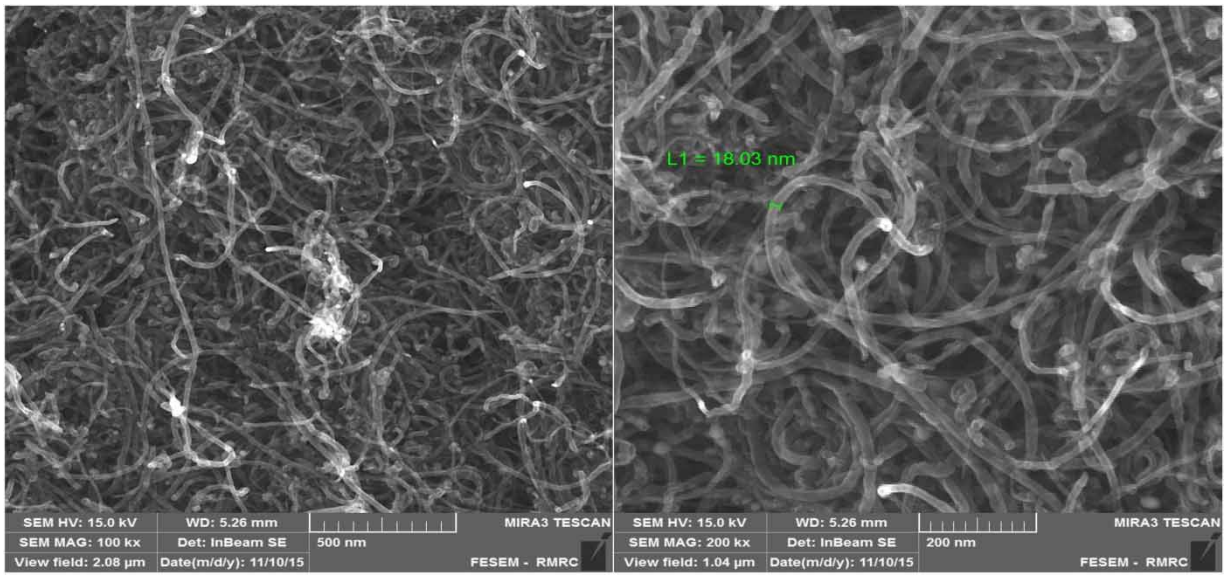


**Figure 2** | SEM images of the MWCNT at different magnifications.

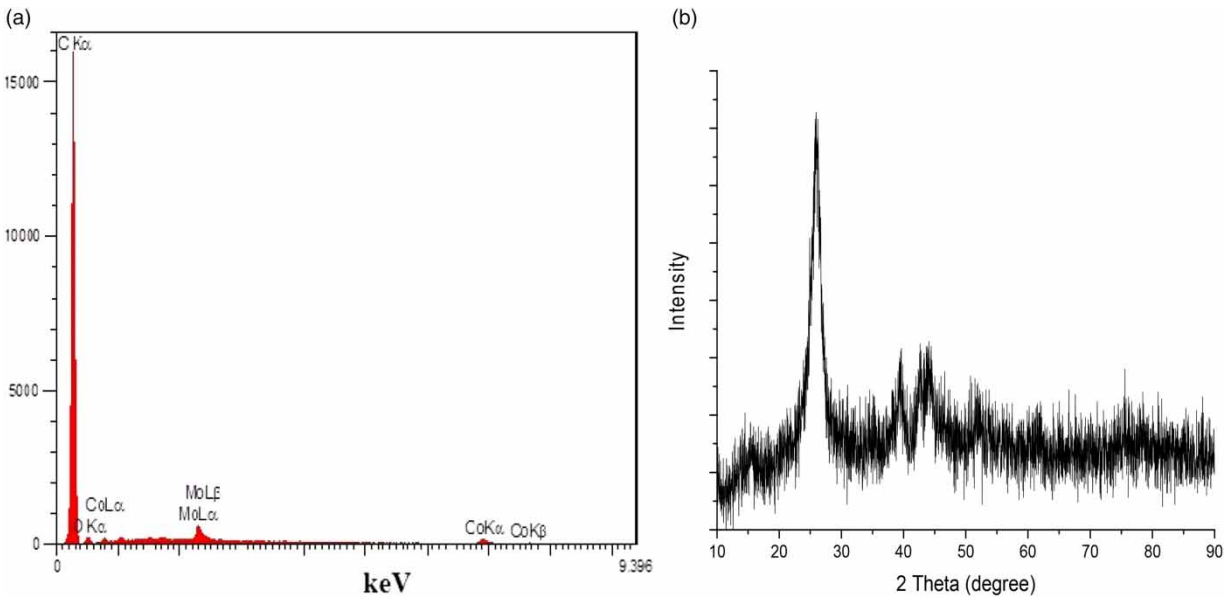


**Figure 3** | EDS spectrum (a) and XRD pattern (b) of the MWCNT.

**Table 2** | Quantitative results of EDS analysis of the MWCNT

| Element | Line | Intensity | Kr | Wt% | Atom% |
|---|---|---|---|---|---|
| C | Ka | 1,138.1 | 0.7234 | 90.98 | 96.05 |
| O | Ka | 17.3 | 0.0055 | 3.92 | 3.11 |
| Co | Ka | 22.2 | 0.0151 | 2.07 | 0.45 |
| Mo | La | 70.5 | 0.0234 | 3.03 | 0.40 |
| Total | – | – | 0.7673 | 100.00 | 100.00 |

**Table 3** | Textural properties of the adsorbent

| Adsorbent | Surface area ($m^2/g$) | Total pore volume ($cm^3/g$) | Average pore diameter (nm) |
|---|---|---|---|
| MWCNT | 221.908 | 0.716 | 2.722 |

is increased from 5 to 11 (Figure 4). The relationship between the solution pH and TC adsorption can be explained by considering both the surface charges and properties of the adsorbent

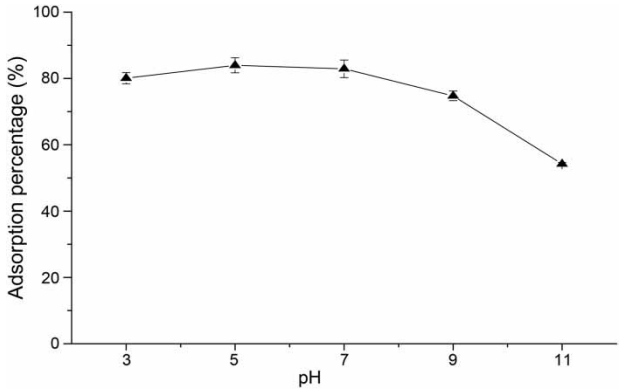


**Figure 4** | Effect of pH on the adsorption of TC onto MWCNT. Condition: temperature 20 °C; initial TC concentration 50 mg $L^{-1}$; adsorbent dosage 0.5 g $L^{-1}$.

and the pH-dependent speciation of TC antibiotic. Changing the solution pH cannot only affect the protonation–deprotonation transition of functional groups on an adsorbent but also can result in a change in chemical speciation of organic compounds (Zhang *et al.* 2011b). TC (symbolized as $H_2L$) is an amphoteric molecule having multiple ionizable functional groups (such as amino, phenol, and alcohol) depending on the solution pH. Since TC has three pKa values (3.30, 7.68 and 9.68), it exists as cation ($H_3L^+$) due to the protonation of dimethyl-ammonium group when solution pH is below 3.3. At pH between 3.3 and 7.68, TC exists as a zwitterion ($H_2L^0$) due to the loss of a proton from the phenolic diketone moiety. At solution pH greater than 7.68, TC exists as anions ($HL^{-1}$ and $L^{-2}$) because of the loss of protons from the tri-carbonyl system and phenolic diketone moiety (Kang *et al.* 2011; Zhang *et al.* 2011b). At pH between 3.3 and 7.7, the most dominant adsorption mechanism is probably the non-electrostatic π-π dispersion interaction between bulk π systems on the MWCNT surface and TC molecules contained both benzene rings and double bonds (C=C, C=O), or hydrophobic interaction between the MWCNT and TC (Zhang *et al.* 2011b). In this pH range, TC exists as zwitterion, nearly all TC molecules carry no net electrical charge, and there is almost no electrostatic attraction or repulsion between TC molecules and the adsorbent. Thus, the increase of pH from 5 to 7 has no remarkable influence on the adsorption affinity of TC onto the MWCNT. However, the reduced TC adsorption at pH < 3.3 and pH > 7.7 can be justified by the increased formation of $H^+$ or $OH^-$ in the solution at the related pH. At pH above 9, the surface of the MWCNT is negatively charged; therefore, the electrostatic repulsion between the surface of the adsorbent and TC species ($HL^-$ and $L^{2-}$) reduces the TC adsorption (Yu *et al.* 2014a). It should be noted that the pH of the solutions was not fixed for the rest of our experiments since the pH of the prepared working solutions was in the range of 4–5, in which TC molecules are dominantly present as zwitterion. The results of the present study are consistent with the results of other researchers. For instance, Rivera-Utrilla *et al.* (2013) reported that the adsorption of TC on the activated carbon remained constant in the pH range of 2–7 and decreased as the pH was increased. Zhang *et al.* (2011c) also stated that the adsorption of TC on soil and sediment was relatively constant at pH 5–9 and decreased at pH > 9.

## Effect of adsorbent dosage

Adsorbent dosage is another important parameter in the determination of adsorption capacity. The effect of the adsorbent dosage was investigated for the initial TC concentration of 50 mg $L^{-1}$ and 100 mg $L^{-1}$ by adding various amounts of MWCNT to TC solutions. Figure 5(a) and 5(b) show the adsorption percentage and the amount of TC adsorbed as a function of the MWCNT dosage, respectively. The increase in the percentage of TC removal with increasing adsorbent dosage could be attributed to the increase in the adsorbent surface area, which increases the number of adsorption sites available for adsorption, as already reported in the literature (Cardoso *et al.* 2011). On the other hand, by increasing the adsorbent dosage, the amounts of TC adsorbed onto the MWCNT decreases remarkably (Figure 5(b)). This phenomenon can be explained through two aspects. First, at a fixed concentration and volume of TC, the increase of the adsorbent dosage will lead to unsaturation of adsorption sites through the adsorption process; second, the particle aggregation due to higher mass of the adsorbent may result in a reduction in the adsorbent capacity. Therefore, such aggregation would lead to a decrease in the total surface area of the adsorbent and an increase in the diffusional path length (Cardoso *et al.* 2011).

## Effect of cations and anions

The effects of background cations ($Li^+$, $K^+$, $Mg^{2+}$, $Ni^{2+}$ and $Fe^{3+}$) and anions ($HCO_3^-$, $NO_3^-$, and $SO_4^{2-}$) on the adsorption of TC onto the MWCNT were investigated using batch adsorption experiments, and the results are shown in Figure 6. As reported in the literature, the concentration of anions such as nitrate, bicarbonate, and sulfate and most of cations such as potassium, lithium, calcium, magnesium, and nickel in surface waters is usually less than 1 mM (Hem 1985; Bui & Choi 2010); therefore, we used 1 mM salts of these anions and cations to evaluate their effects on TC adsorption. The adsorption of TC in the presence of the anions and cations was compared to TC

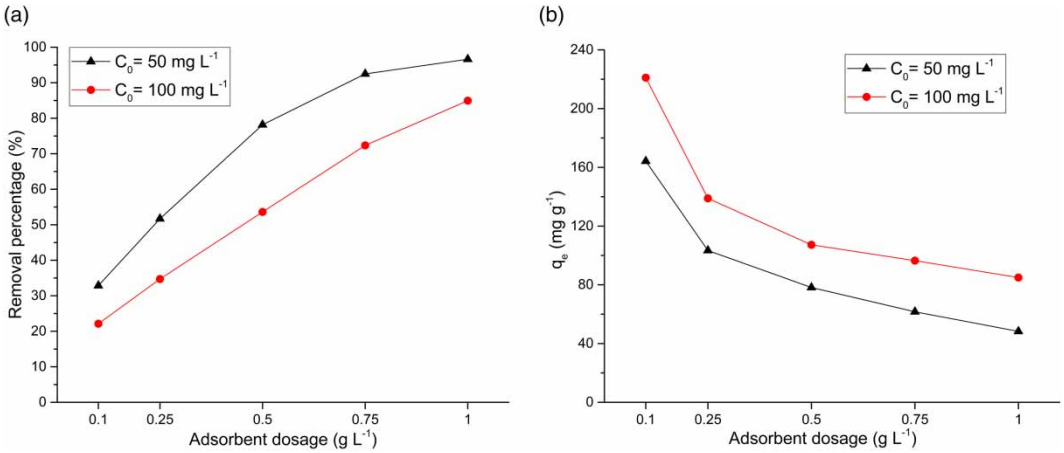


**Figure 5** | Effect of MWCNT dosage on the adsorption of TC: (a) represents removal percentage and (b) represents the amount of TC adsorbed. Conditions: natural pH; temperature 20 °C; contact time 4 h.

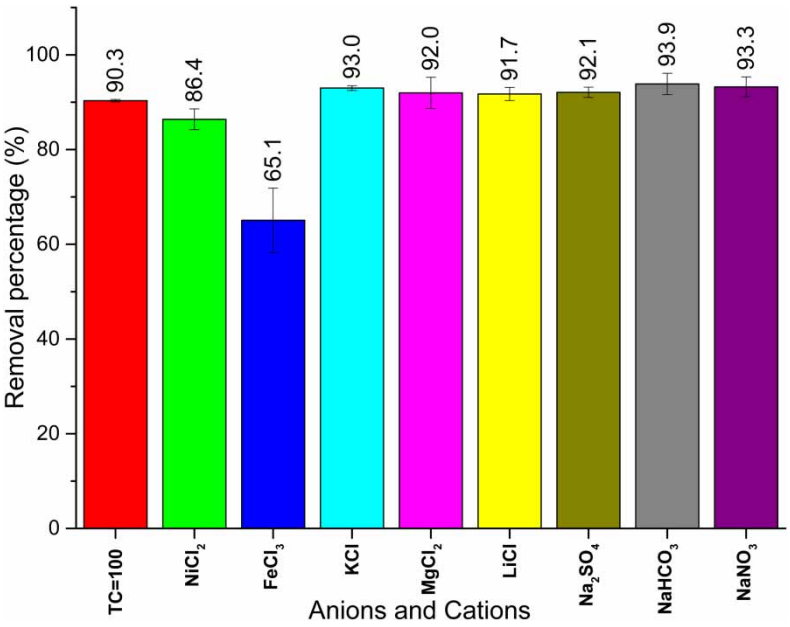


**Figure 6** | The adsorption of TC onto the MWCNT in the presence of 1 mM cations and anions, compared to control (initial TC 100 mg $L^{-1}$). Error bars represent the SD of sample replicates. Conditions: natural pH; temperature 20 °C; contact time 4 h; adsorbent dosage 1 g $L^{-1}$.

adsorption in the absence of the tested anions and cations (sample containing only the adsorbent and 100 mg $L^{-1}$ TC). The ANOVA test results indicated that the tested anions and the monovalent and divalent cations did not significantly affect TC adsorption ($p > 0.05$). However, the presence of $Ni^{2+}$ slightly decreases TC adsorption (Figure 6); this slight decrease can be considered as a competition of $Ni^{2+}$ with TC species to adsorb on active sites of the adsorbent. On the other hand, the presence of the other anions and cations (except $Fe^{3+}$) slightly increases TC adsorption onto the MWCNT (Figure 6); this increase in the adsorption may be attributed to surface bridging mechanism and the formation of surface complexes on the surface sites (Zhao *et al.* 2011). On the contrary, the presence of $Fe^{3+}$ significantly affected and decreased the adsorption of TC ($p < 0.05$). This decrease in the adsorption of TC onto the MWCNT may be attributed to the highest tendency of $Fe^{3+}$ to adhere to the negatively charged oxidized MWCNTs, which in turn reduces ion interaction sites (or available sites) on the surface of the oxidized MWCNT for TC adsorption. The results of this study are in good agreement with the results of the other researchers. For

instance, Liu *et al.* (2012a) investigated the removal of TC from water by Fe-Mn binary oxide and reported that the presence of cations and anions such as $Ca^{2+}$, $Mg^{2+}$, $CO_3^{2-}$ and $SO_4^{2-}$ had no significant effect on the TC removal in their experimental conditions, while $SiO_3^{2-}$ and $PO_4^{3-}$ hindered the adsorption of TC. Zhao *et al.* (2011) evaluated the adsorption of TC onto goethite in the presence of metal cations and humic substances. They stated that at the studied pH range, the presence of five background electrolyte cations ($Li^+$, $Na^+$, $K^+$, $Ca^{2+}$, and $Mg^{2+}$) with a concentration of 0.01 M had little effect on the TC adsorption. The adsorption of four pharmaceuticals (carbamazepine, diclofenac, ibuprofen, and ketoprofen) to silica as a function of ionic strength, anions, cations, and natural organic matter was investigated by Bui & Choi (2010). The authors reported that the tested anions did not significantly affect the adsorption of these pharmaceuticals to silica ($p > 0.05$). Their results also showed that divalent cations did not significantly affect the adsorption of carbamazepine and diclofenac; however, divalent cations at low concentrations (1 mM) increased the adsorption of ibuprofen and ketoprofen. In contrast with the present study, in that study the presence of $Fe^{3+}$ significantly increased the adsorption of the pharmaceuticals, but in our study it significantly decreased the adsorption of TC. This difference may be ascribed to the different structures of both adsorbate and adsorbent used in the studies. Blank experiments were also run for both anions and cations at the same conditions to observe the changes in the initial concentration of TC because of possible reactions between TC and the tested anions and cations. The change in TC concentration in the blank samples was in the range of 0.2–2% for all cations and anions.

## Kinetic studies

In the treatment of aqueous effluents by adsorption process, it is important to evaluate adsorption kinetics because they provide valuable pieces of information on the reaction pathways as well as on the mechanisms of the adsorption process (Cardoso *et al.* 2011). The kinetic plots for the adsorption of TC onto the MWCNT are shown in Figure 7. The fitting parameters of the kinetic models are presented in Table 4. In addition to the adjusted $R^2$ value, the SD value was also used to explain the suitability of the fitted models as we fitted the experimental data to the nonlinear kinetic models. A higher SD value indicates that a higher deviation exists between q value calculated theoretically by the model and q value measured experimentally. It has been reported in the literature (Prola *et al.* 2013) that the best fit of the data is a function of the number of parameters in nonlinear models. Therefore, due to this fact, we considered the number of parameters of each model (p term in Equation (15)) for calculating the SD values and evaluating the kinetic models. The minimum SD value was used to divide the SD value of each model (SD ratio); and, subsequently, the fitness of each model was compared based on the SD ratio value. For the initial TC concentration of 75 and 100 mg $L^{-1}$, the lowest SD values were obtained for the Avrami-fractional-order kinetic model. In this work, for TC concentration of 75 mg $L^{-1}$, the SD ratio values for the pseudo-first-order, pseudo-second-order, and general order kinetic models were 5.19, 1.47, and 1.17, respectively, while the corresponding values for TC concentration of 100 mg $L^{-1}$ were 3.95, 1.56, and 1.54, respectively. The results obtained by the fitted models clearly showed that the Avrami-fractional order kinetic model better explained the adsorption of TC onto the MWCNT because this model exhibited the SD ratio value of 1.00, which is a lower value when compared to the other kinetic models. Additionally, this model showed the highest $R^2_{adj}$ value, as well as the $q_e$ values predicted by the fractionary-order were closer to the experimental $q_e$ values. It can be found in the literature that several kinetic processes of different adsorbents and adsorbates have been successfully explained by the Avrami kinetic equation (Cardoso *et al.* 2011). The Avrami exponent, $n_{AV}$, is a fractionary number, which is associated with the possible changes in the adsorption mechanism during the adsorption process. Instead of following only an integer-kinetic order, the adsorption mechanism could follow multiple kinetic orders, which change during the contact of an adsorbate with an adsorbent (Royer *et al.* 2009). The $n_{AV}$ exponent is achieved from the multiple kinetic orders of an adsorption process. As mentioned, the Avrami kinetic model fit better our experimental data; therefore, we used the intra-particle diffusion model to investigate the influence of mass transfer resistance on the binding of TC to the adsorbent, MWCNT (see Table 3 and Figure 6(c) and 6(d)). Intra-particle diffusion constant ($k_{id}$) in terms of mg $g^{-1}$ $min^{-0.5}$ can be obtained from the slope of the plot of $q_t$ (the amount adsorbed at any time) versus the square root of time. The plots of $q_t$ versus $t^{0.5}$ are shown in Figure 7(c) and 7(d) for the two initial TC concentrations. The plots have three linear sections indicating that the adsorption process follows more than one adsorption rate (Ribas *et al.* 2014). Each linear can be attributed to each stage of

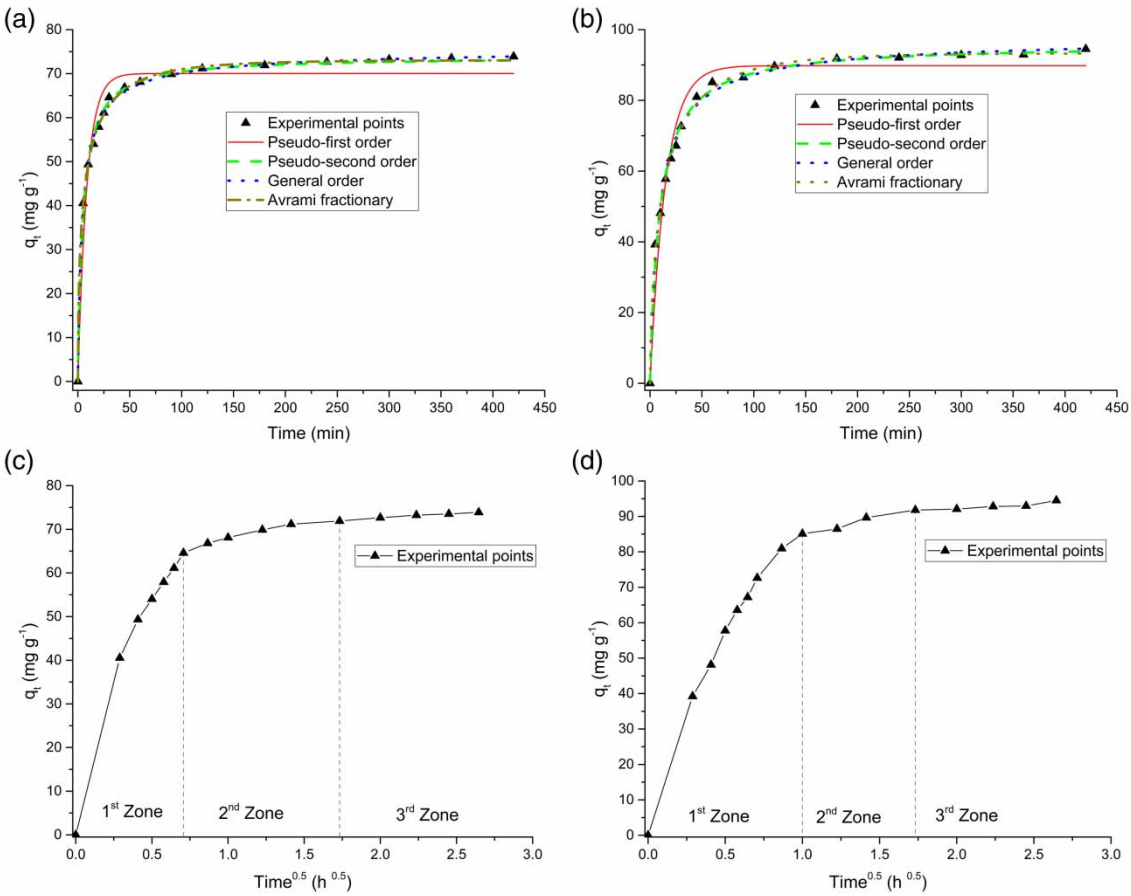


**Figure 7** | Kinetic curves for the adsorption of TC onto the MWCNT at 20 °C: (a) $C_o = 75$ mg L$^{-1}$; (b) $C_o = 100$ mg L$^{-1}$; (c) intra-particle diffusion for $C_o = 75$ mg L$^{-1}$; (d) intra-particle diffusion for $C_o = 100$ mg L$^{-1}$. Conditions: natural pH; adsorbent dosage 1 g L$^{-1}$.

the adsorption process. Accordingly, the process in which TC molecules diffuse to the surface of the adsorbent can be referred to the first linear section, which is the fastest sorption stage (Ribas *et al.* 2014). The second linear section is a delayed process and can be attributed to the intra-particle diffusion (Ribas *et al.* 2014). The third portion is obtained after the equilibrium and describes diffusion through smaller pores (Ribas *et al.* 2014). The kinetic studies reveal that the minimum contact time to reach the equilibrium for the adsorption of TC onto the MWCNT is about 120 min. For the rest of our experimental work, the contact time was fixed at 240 min to ensure that the equilibrium would be attained between the adsorbate even at higher concentrations and MWCNT as the adsorbent (Cardoso *et al.* 2011).

## Equilibrium studies

Adsorption isotherms describe how the adsorbate molecules distribute between the liquid phase and the solid phase when the adsorption process reaches an equilibrium state. In other words, adsorption isotherms are used to describe the relationship between the amount of adsorbate adsorbed by the adsorbent ($q_e$) and the adsorbate concentration remaining in the solution after the system has reached to the equilibrium state ($C_e$) at a constant temperature. In addition, some information about adsorption mechanism, the affinity of the adsorbate to the adsorbent, and surface properties can be obtained from the adsorption parameters of equilibrium models. In this study, the isotherms of adsorption of TC onto the MWCNT were carried out at 20 °C using the optimum experimental condition described previously. Figure 8 shows the adsorption isotherms of TC onto the MWCNT. The parameters predicted by the nonlinear adsorption models are presented in Table 5. Based on the SD values, it is clear that the Liu model best describes the equilibrium data since this model shows the lowest SD value. The SD ratio was used to compare the studied isotherm models. The procedure used for

**Table 4** | Kinetic parameters obtained from the nonlinear models for the adsorption of TC onto the MWCNT

| | TC concentration mg $L^{-1}$ | |
|---|---|---|
| **Kinetic model** | **75** | **100** |
| *Pseudo-first-order* | | |
| $K_f$ ($min^{-1}$) | 0.1162 | 0.06691 |
| $q_e$ (mg $g^{-1}$) | 70.03 | 89.82 |
| $h_0$ (mg $g^{-1}$ $min^{-1}$) | 8.138 | 6.011 |
| SD (mg $g^{-1}$) | 4.075 | 5.089 |
| $R^2_{adj}$ | 0.9532 | 0.9614 |
| *Pseudo-second-order* | | |
| $K_s$ (g $mg^{-1}$ $min^{-1}$) | $2.821.10^{-3}$ | $1.119.10^{-3}$ |
| $q_e$ (mg $g^{-1}$) | 73.83 | 95.93 |
| $h_0$ (mg $g^{-1}$ $min^{-1}$) | 15.38 | 10.30 |
| SD (mg $g^{-1}$) | 1.158 | 2.014 |
| $R^2_{adj}$ | 0.9962 | 0.9940 |
| *General order* | | |
| $K_N$ [$h^{-1}$(g $mg^{-1}$)$^{n-1}$] | $5.541.10^{-4}$ | $3.560.10^{-4}$ |
| $q_e$ (mg $g^{-1}$) | 76.07 | 98.30 |
| n | 2.415 | 2.261 |
| $h_0$ (mg $g^{-1}$ $min^{-1}$) | 19.39 | 11.50 |
| SD (mg $g^{-1}$) | 0.9190 | 1.986 |
| $R^2_{adj}$ | 0.9976 | 0.9941 |
| *Avrami fractionary* | | |
| $K_{Av}$ ($min^{-1}$) | 0.1288 | 0.064141 |
| $q_e$ (mg $g^{-1}$) | 73.08 | 93.32 |
| $n_{AV}$ | 0.4973 | 0.5958 |
| $h_0$ (mg $g^{-1}$ $min^{-1}$) | 9.414 | 5.986 |
| SD (mg $g^{-1}$) | 0.7851 | 1.288 |
| $R^2_{adj}$ | 0.9983 | 0.9975 |
| *Intra-particle diffusion* | | |
| $k_{id}$ (mg $g^{-1}$ $min^{-0.5}$)[a] | 5.080 | 3.460 |
| $R^2$ | 0.9495 | 0.9523 |

Conditions: temperature 20 °C; pH natural; adsorbent dosage 1 g $L^{-1}$.
[a]Second zone.

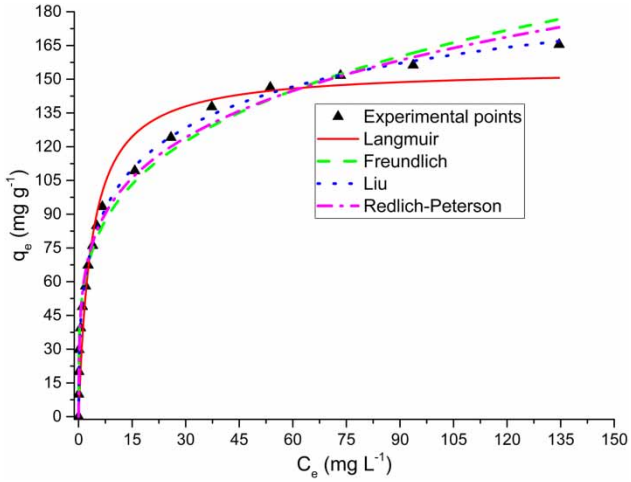


**Figure 8** | Isotherm curves for the adsorption of TC onto the MWCNT at 20 °C. Conditions: natural pH; adsorbent dosage 1 g $L^{-1}$, contact time between the adsorbent and the adsorbate 4 h.

**Table 5** | Isotherm parameters for the adsorption of TC onto the MWCNT adsorbent

| **Isotherm model** | **Parameter** | **Value** |
|---|---|---|
| Langmuir | $Q_{max}$ (mg $g^{-1}$) | 154.7 |
| | $K_L$ (L $mg^{-1}$) | 0.2743 |
| | $R^2_{adj}$ | 0.9501 |
| | SD (mg $g^{-1}$) | 12.04 |
| Freundlich | $K_F$ [mg $g^{-1}$ (mg $L^{-1}$)$^{-1/n}_F$] | 53.27 |
| | $n_F$ | 4.089 |
| | $R^2_{adj}$ | 0.9857 |
| | SD (mg $g^{-1}$) | 6.452 |
| Liu | $Q_{max}$ (mg $g^{-1}$) | 253.4 |
| | $K_g$ (L $mg^{-1}$) | 0.03556 |
| | $n_L$ | 0.4203 |
| | $R^2_{adj}$ | 0.9968 |
| | SD (mg $g^{-1}$) | 3.025 |
| Redlich–Peterson | $K_{RP}$ L $g^{-1}$ | 561.5 |
| | $a_{RP}$ (mg $L^{-1}$)$^{-g}$ | 9.434 |
| | g | 0.7818 |
| | $R^2_{adj}$ | 0.9903 |
| | SD (mg $g^{-1}$) | 5.302 |

Conditions: adsorbent dosage 1 g $L^{-1}$; natural pH; temperature 20 °C, and contact time 4 h.

calculating the SD ratio is described in the previous section (kinetic studies). The SD values of the Langmuir, Freundlich, and Redlich–Peterson models are 3.98, 2.14, and 1.75 times higher than the SD value obtained for the Liu model (Table 5). The maximum amount of TC adsorbed onto the MWCNT ($Q_{max}$) predicted by the Liu model is 253.38 mg $g^{-1}$, indicating this adsorbent is a good adsorbent for the removal of TC from aqueous solutions. It can be obviously seen from Figure 8 that with increasing the initial TC concentration from 10 to 300 mg $L^{-1}$, the amount of TC adsorbed onto the MWCNT increases from 9.99 to 165.4 mg $g^{-1}$, while the removal percentage decreases from 99.9% to 53.1%. To compare the efficiency of the MWCNT used in this work with other adsorbents, the maximum adsorption capacity of different adsorbents for the removal of TC is presented in Table 6. The values of $Q_{max}$ were

**Table 6** | Maximum sorption capacity of different adsorbents used for the adsorption of TC

| Adsorbent | $Q_{max}$ (mg $g^{-1}$) | Reference |
|---|---|---|
| Carbon nanotubes (MWCNT) | 253.38 | Present study |
| Montmorillonite | 250 | Zhao *et al.* (2012) |
| Chitosan | 23.92 | Kang *et al.* (2010) |
| Fe–$TiO_2$–PPy | 149.25 | Thayyath *et al.* (2015) |
| Zeolite beta | 75.55 | Kang *et al.* (2011) |
| Graphene oxide | 313.480 | Gao *et al.* (2012) |
| CNTs-3.2%O | 269.25 | Yu *et al.* (2014a) |
| Bamboo charcoal | 22.7 | Liao *et al.* (2013) |
| Alkali bio-char | 58.8 | Liu *et al.* (2012b) |
| PC-based AC | 1121.5 | Zhang *et al.* (2015) |
| NaOH-activated carbon | 455.8 | Martins *et al.* (2015) |

obtained at the best experimental conditions of each work.

## CONCLUSIONS

The adsorption of TC antibiotic onto the oxidized MWCNT as a novel adsorbent was carried out by using a batch adsorption technique. The effects of different operational parameters such as pH of solution, adsorbent dosage, background electrolytes, contact time, and initial TC concentration were evaluated. The optimum pH for TC adsorption was in the range of 5–7 and the adsorption reached the equilibrium after about 120 min. The ANOVA test results show that all the studied cations and anions (except $Fe^{3+}$) did not significantly affect the adsorption of TC onto the MWCNT. The TC antibiotic interacted with the oxidized MWCNT at the solid/liquid interface as it suspended in water. The experimental data were fitted to four nonlinear kinetic models, and the Avrami fractionary-order kinetic model best described the kinetic of TC adsorption. However, the intra-particle diffusion model gave multiple linear regions suggesting that the adsorption could also follow multiple adsorption rates. Equilibrium data were fitted to four known isotherm models, and the Liu model gave the best fit with the maximum adsorption capacity of 253.38 mg $g^{-1}$. The results of the present study indicate that oxidized MWCNT can be a good alternative adsorbent for the removal of TC and other pollutants from aqueous solutions.

## ACKNOWLEDGEMENTS

The authors are grateful to the Vice Chancellery for Research Development and Technology of Ahvaz Jundishapur University of Medical Sciences, and Environmental Technologies Research Center (ETRC) for funding and providing necessary facilities to accomplish this research with project number of ETRC-9209. In addition, the authors are also grateful to the National Council for Scientific and Technological Development (CNPq, Brazil).

## REFERENCES

Alavi, N., Babaei, A., Shirmardi, M., Naimabadi, A. & Goudarzi, G. 2015 Assessment of oxytetracycline and tetracycline antibiotics in manure samples in different cities of Khuzestan Province, Iran. *Environmental Science and Pollution Research* **22** (22), 17948–17954.

Babaei, A. A., Azari, A., Kalantary, R. R. & Kakavandi, B. 2015 Enhanced removal of nitrate from water using nZVI@MWCNTs composite: synthesis, kinetics and mechanism of reduction. *Water Science & Technology* **72** (11), 1988–1999.

Bui, T. X. & Choi, H. 2010 Influence of ionic strength, anions, cations, and natural organic matter on the adsorption of pharmaceuticals to silica. *Chemosphere* **80** (7), 681–686.

Cardoso, N. F., Pinto, R. B., Lima, E. C., Calvete, T., Amavisca, C. V., Royer, B., Cunha, M. L., Fernandes, T. H. M. & Pinto, I. S. 2011 Removal of remazol black B textile dye from aqueous solution by adsorption. *Desalination* **269** (1–3), 92–103.

Chaudhary, K. T., Ali, J. & Yupapin, P. P. 2014 Growth of small diameter multi-walled carbon nanotubes by arc discharge process. *Chinese Physics B* **23** (3), 035203.

Dehghani, M. H., Naghizadeh, A., Rashidi, A. & Derakhshani, E. 2013 Adsorption of reactive blue 29 dye from aqueous solution by multiwall carbon nanotubes. *Desalination and Water Treatment* **51** (40–42), 7655–7662.

Derakhshani, E. & Naghizadeh, A. 2013 Ultrasound regeneration of multi wall carbon nanotubes saturated by humic acid. *Desalination and Water Treatment* **52** (40–42), 7468–7472.

Freundlich, H. 1906 Adsorption in solution. *Phys. Chem. Soc.* **40**, 1361–1368.

Gao, Y., Li, Y., Zhang, L., Huang, H., Hu, J., Shah, S. M. & Su, X. 2012 Adsorption and removal of tetracycline antibiotics from aqueous solution by graphene oxide. *Journal of Colloid and Interface Science* **368** (1), 540–546.

Hem, J. D. 1985 *Study and Interpretation of the Chemical Characteristics of Natural Water*. Department of the Interior, US Geological Survey, Washington, DC, USA.

Ho, Y.-S. 2006 Review of second-order models for adsorption systems. *Journal of Hazardous Materials* **136** (3), 681–689.

Homem, V. & Santos, L. 2011 Degradation and removal methods of antibiotics from aqueous matrices – a review. *Journal of Environmental Management* **92** (10), 2304–2347.

Jaafarzadeh, N., Kakavandi, B., Takdastan, A., Kalantary, R. R., Azizi, M. & Jorfi, S. 2015 Powder activated carbon/$Fe_3O_4$ hybrid composite as a highly efficient heterogeneous catalyst for Fenton oxidation of tetracycline: degradation mechanism and kinetic. *RSC Advances* **5** (103), 84718–84728.

Ji, L., Chen, W., Duan, L. & Zhu, D. 2009 Mechanisms for strong adsorption of tetracycline to carbon nanotubes: a comparative study using activated carbon and graphite as adsorbents. *Environmental Science & Technology* **43** (7), 2322–2327.

Kakavandi, B., Esrafili, A., Mohseni-Bandpi, A., Jonidi Jafari, A. & Rezaei Kalantary, R. 2014 Magnetic $Fe_3O_4$@C nanoparticles as adsorbents for removal of amoxicillin from aqueous solution. *Water Science & Technology* **69** (1), 147–155.

Kakavandi, B., Takdastan, A., Jaafarzadeh, N., Azizi, M., Mirzaei, A. & Azari, A. 2016 Application of $Fe_3O_4$@C catalyzing heterogeneous UV-Fenton system for tetracycline removal with a focus on optimization by a response surface method. *Journal of Photochemistry and Photobiology A: Chemistry* **314**, 178–188.

Kang, J., Liu, H., Zheng, Y.-M., Qu, J. & Chen, J. P. 2010 Systematic study of synergistic and antagonistic effects on adsorption of tetracycline and copper onto a chitosan. *Journal of Colloid and Interface Science* **344** (1), 117–125.

Kang, J., Liu, H., Zheng, Y.-M., Qu, J. & Chen, J. P. 2011 Application of nuclear magnetic resonance spectroscopy, Fourier transform infrared spectroscopy, UV–Visible spectroscopy and kinetic modeling for elucidation of adsorption chemistry in uptake of tetracycline by zeolite beta. *Journal of Colloid and Interface Science* **354** (1), 261–267.

Kyzas, G. Z., Koltsakidou, A., Nanaki, S. G., Bikiaris, D. N. & Lambropoulou, D. A. 2015 Removal of beta-blockers from aqueous media by adsorption onto graphene oxide. *Science of the Total Environment* **537**, 411–420.

Langmuir, I. 1918 The adsorption of gases on plane surfaces of glass, mica and platinum. *Journal of the American Chemical Society* **40** (9), 1361–1403.

Liao, P., Zhan, Z., Dai, J., Wu, X., Zhang, W., Wang, K. & Yuan, S. 2013 Adsorption of tetracycline and chloramphenicol in aqueous solutions by bamboo charcoal: a batch and fixed-bed column study. *Chemical Engineering Journal* **228**, 496–505.

Liu, Y. & Liu, Y.-J. 2008 Biosorption isotherms, kinetics and thermodynamics. *Separation and Purification Technology* **61** (3), 229–242.

Liu, Y. & Shen, L. 2008 A general rate law equation for biosorption. *Biochemical Engineering Journal* **38** (3), 390–394.

Liu, Y., Xu, H., Yang, S.-F. & Tay, J.-H. 2003 A general model for biosorption of $Cd^{2+}$, $Cu^{2+}$ and $Zn^{2+}$ by aerobic granules. *Journal of Biotechnology* **102** (3), 233–239.

Liu, H., Yang, Y., Kang, J., Fan, M. & Qu, J. 2012a Removal of tetracycline from water by Fe-Mn binary oxide. *Journal of Environmental Sciences* **24** (2), 242–247.

Liu, P., Liu, W. J., Jiang, H., Chen, J. J., Li, W. W. & Yu, H. Q. 2012b Modification of bio-char derived from fast pyrolysis of biomass and its application in removal of tetracycline from aqueous solution. *Bioresource Technology* **121**, 235–240.

Ma, J., Yang, M., Yu, F. & Zheng, J. 2015 Water-enhanced removal of ciprofloxacin from water by porous graphene hydrogel. *Scientific Reports* **5**, 13578.

Machado, F. M., Bergmann, C. P., Lima, E. C., Royer, B., de Souza, F. E., Jauris, I. M., Calvete, T. & Fagan, S. B. 2012 Adsorption of Reactive Blue 4 dye from water solutions by carbon nanotubes: experiment and theory. *Physical Chemistry Chemical Physics* **14** (31), 11139–11153.

Martins, A. C., Pezoti, O., Cazetta, A. L., Bedin, K. C., Yamazaki, D. A. S., Bandoch, G. F. G., Asefa, T., Visentainer, J. V. & Almeida, V. C. 2015 Removal of tetracycline by NaOH-activated carbon produced from macadamia nut shells: kinetic and equilibrium studies. *Chemical Engineering Journal* **260**, 291–299.

Mohan, D., Rajput, S., Singh, V. K., Steele, P. H. & Pittman Jr, C. U. 2011 Modeling and evaluation of chromium remediation from water using low cost bio-char, a green adsorbent. *Journal of Hazardous Materials* **188** (1–3), 319–333.

Morsy, M., Helal, M., El-Okr, M. & Ibrahim, M. 2014 Preparation, purification and characterization of high purity multi-wall carbon nanotube. *Spectrochimica Acta Part A: Molecular and Biomolecular Spectroscopy* **132**, 594–598.

Prola, L. D. T., Machado, F. M., Bergmann, C. P., de Souza, F. E., Gally, C. R., Lima, E. C., Adebayo, M. A., Dias, S. L. P. & Calvete, T. 2013 Adsorption of Direct Blue 53 dye from aqueous solutions by multi-walled carbon nanotubes and activated carbon. *Journal of Environmental Management* **130**, 166–175.

Redlich, O. & Peterson, D. L. 1959 A useful adsorption isotherm. *Journal of Physical Chemistry* **63** (6), 1024–1024.

Ribas, M. C., Adebayo, M. A., Prola, L. D. T., Lima, E. C., Cataluña, R., Feris, L. A., Puchana-Rosero, M. J., Machado, F. M., Pavan, F. A. & Calvete, T. 2014 Comparison of a homemade cocoa shell activated carbon with commercial activated carbon for the removal of reactive violet 5 dye from aqueous solutions. *Chemical Engineering Journal* **248**, 315–326.

Rivera-Utrilla, J., Gómez-Pacheco, C. V., Sánchez-Polo, M., López-Peñalver, J. J. & Ocampo-Pérez, R. 2013 Tetracycline removal from water by adsorption/bioadsorption on activated carbons and sludge-derived adsorbents. *Journal of Environmental Management* **131**, 16–24.

Royer, B., Cardoso, N. F., Lima, E. C., Ruiz, V. S. O., Macedo, T. R. & Airoldi, C. 2009 Organofunctionalized kenyaite for dye removal from aqueous solution. *Journal of Colloid and Interface Science* **336** (2), 398–405.

Safari, G. H., Nasseri, S., Mahvi, A. H., Yaghmaeian, K., Nabizadeh, R. & Alimohammadi, M. 2015 Optimization of sonochemical degradation of tetracycline in aqueous solution using sono-activated persulfate process. *Journal of Environmental Health Science and Engineering* **13**, 76.

Salam, M. A. & Burk, R. 2008 Thermodynamics of pentachlorophenol adsorption from aqueous solutions by oxidized multi-walled carbon nanotubes. *Applied Surface Science* **255** (5), 1975–1981.

Saucier, C., Adebayo, M. A., Lima, E. C., Cataluna, R., Thue, P. S., Prola, L. D., Puchana-Rosero, M. J., Machado, F. M., Pavan, F. A. & Dotto, G. L. 2015a Microwave-assisted activated carbon from cocoa shell as adsorbent for removal of sodium diclofenac and nimesulide from aqueous effluents. *Journal of Hazardous Materials* **289**, 18–27.

Saucier, C., Adebayo, M. A., Lima, E. C., Prola, L. D. T., Thue, P. S., Umpierres, C. S., Rosero, M. J. P. & Machado, F. M. 2015b Comparison of a homemade bacuri shell activated carbon with carbon nanotubes for food dye removal. *CLEAN–Soil, Air, Water* **43**, 1389–1400.

Shirmardi, M., Mesdaghinia, A., Mahvi, A. H., Nasseri, S. & Nabizadeh, R. 2012 Kinetics and equilibrium studies on adsorption of Acid Red 18 (Azo-Dye) using multiwall carbon nanotubes (MWCNTs) from aqueous solution. *Journal of Chemistry* **9** (4), 2371–2383.

Shirmardi, M., Mahvi, A., Hashemzadeh, B., Naeimabadi, A., Hassani, G. & Niri, M. 2013a The adsorption of malachite green (MG) as a cationic dye onto functionalized multi walled carbon nanotubes. *Korean Journal of Chemical Engineering* **30** (8), 1603–1608.

Shirmardi, M., Mahvi, A. H., Mesdaghinia, A., Nasseri, S. & Nabizadeh, R. 2013b Adsorption of acid red 18 dye from aqueous solution using single-wall carbon nanotubes: kinetic and equilibrium. *Desalination and Water Treatment* **51** (34–36), 6507–6516.

Terzopoulou, Z., Papageorgiou, M., Kyzas, G. Z., Bikiaris, D. N. & Lambropoulou, D. A. 2016 Preparation of molecularly imprinted solid-phase microextraction fiber for the selective removal and extraction of the antiviral drug abacavir in environmental and biological matrices. *Analytica Chimica Acta* **913**, 63–75.

Thayyath, S. A., Peethambaran, L. D. & Jayachandran, N. 2015 Utilization of polypyrrole coated iron-doped titania based hydrogel for the removal of tetracycline hydrochloride from aqueous solutions: adsorption and photocatalytic degradation studies. *Environmental Nanotechnology, Monitoring & Management* **4**, 106–117.

Upadhyayula, V. K. K., Deng, S., Mitchell, M. C. & Smith, G. B. 2009 Application of carbon nanotube technology for removal of contaminants in drinking water: a review. *Science of the Total Environment* **408** (1), 1–13.

Vosoughi Niri, M., Shirmardi, M., Asadi, A., Golestani, H., Naeimabadi, A., Mohammadi, M. J. & Heidari Farsani, M. 2014 Reactive red 120 dye removal from aqueous solution by adsorption on nano-alumina. *Journal of Water Chemistry and Technology* **36** (3), 125–133.

Weber, W. J. & Morris, J. C. 1963 Kinetics of adsorption on carbon from solution. *Journal of the Sanitary Engineering Division* **89** (2), 31–60.

Yu, F., Ma, J. & Han, S. 2014a Adsorption of tetracycline from aqueous solutions onto multi-walled carbon nanotubes with different oxygen contents. *Scientific Reports* **4**, 5326.

Yu, F., Sun, S., Han, S., Zheng, J. & Ma, J. 2016 Adsorption removal of ciprofloxacin by multi-walled carbon nanotubes with different oxygen contents from aqueous solutions. *Chemical Engineering Journal* **285**, 588–595.

Yu, J. G., Zhao, X. H., Yang, H., Chen, X. H., Yang, Q., Yu, L. Y., Jiang, J. H. & Chen, X. Q. 2014b Aqueous adsorption and removal of organic contaminants by carbon nanotubes. *Science of the Total Environment* **482–483**, 241–251.

Zhang, D., Pan, B., Wu, M., Wang, B., Zhang, H., Peng, H., Wu, D. & Ning, P. 2011a Adsorption of sulfamethoxazole on functionalized carbon nanotubes as affected by cations and anions. *Environmental Pollution* **159** (10), 2616–2621.

Zhang, D., Yin, J., Zhao, J., Zhu, H. & Wang, C. 2015 Adsorption and removal of tetracycline from water by petroleum coke-derived highly porous activated carbon. *Journal of Environmental Chemical Engineering* **3** (3), 1504–1512.

Zhang, L., Song, X., Liu, X., Yang, L., Pan, F. & Lv, J. 2011b Studies on the removal of tetracycline by multi-walled carbon nanotubes. *Chemical Engineering Journal* **178**, 26–33.

Zhang, Z., Sun, K., Gao, B., Zhang, G., Liu, X. & Zhao, Y. 2011c Adsorption of tetracycline on soil and sediment: effects of pH and the presence of Cu(II). *Journal of Hazardous Materials* **190** (1–3), 856–862.

Zhao, Y., Geng, J., Wang, X., Gu, X. & Gao, S. 2011 Adsorption of tetracycline onto goethite in the presence of metal cations and humic substances. *Journal of Colloid and Interface Science* **361** (1), 247–251.

Zhao, Y., Gu, X., Gao, S., Geng, J. & Wang, X. 2012 Adsorption of tetracycline (TC) onto montmorillonite: cations and humic acid effects. *Geoderma* **183–184**, 12–18.

First received 19 March 2016; accepted in revised form 3 June 2016. Available online 22 June 2016